doi.org/10.26434/chemrxiv.7364225.v1

Selective Generation of Singlet Oxygen in Chloride Accelerated Copper Fenton Chemistry

Andrew Carrier, Collins Nganou, David Oakley, Yongli Chen, Ken Oakes, Stephanie MacQuarrie, Xu Zhang

Submitted date: 20/11/2018 • Posted date: 20/11/2018

Citation information: Carrier, Andrew; Nganou, Collins; Oakley, David; Chen, Yongli; Oakes, Ken; MacQuarrie, Stephanie; et al. (2018): Selective Generation of Singlet Oxygen in Chloride Accelerated Copper Fenton Chemistry. ChemRxiv. Preprint.

Singlet oxygen ($^1O_2$), a widely used reactive oxygen species (ROS) in industry and biomedical applications, plays a fundamental role throughout nature. We report a novel method to generate $^1O_2$selectively and efficiently through copper-based Fenton chemistry under circumneutral conditions enhanced by chloride as co-catalyst, with reactivity completely different than that observed in classical iron-based Fenton chemistry. The mechanism of its formation was elucidated through the kinetic studies of orthogonally reactive reporter molecules, i.e., singlet oxygen sensor green, 4-hydroxy-2,2,6,6-tetramethylpiperidine, and phenol, and selective ROS quenchers. This method selectively generates $^1O_2$in situneither relying on photosensitization nor resulting in side reactions, and together with the mechanistic understanding of the Cu-Fenton reaction, not only opens new possibilities in many industries, such as organic synthesis and antimicrobial treatments, but also provides insight into Cu and H_2O_2containing chemical, environmental, and biological systems.

Selective Generation of Singlet Oxygen in Chloride Accelerated Copper Fenton Chemistry

Andrew J. Carrier,[a] Collins Nganou,[a] David Oakley,[a] Yongli Chen,[b] Ken Oakes,[c] Stephanie L. MacQuarrie,[d] and Xu Zhang*[a]

[a]Verschuren Centre for Sustainability in Energy and the Environment, Cape Breton University, Sydney, Nova Scotia, B1P 6L2, Canada

[b]Postdoctoral Innovation Practice Base, Shenzhen Polytechnic, Shenzhen, 518055, China

[c]Department of Biology and [d]Department of Chemistry, Cape Breton University, Sydney, Nova Scotia, B1P 6L2, Canada

*Corresponding Author. E-mail: Xu_Zhang@cbu.ca

Abstract

Singlet oxygen ($^1O_2$), a widely used reactive oxygen species (ROS) in industry and biomedical applications, plays a fundamental role throughout nature. We report a novel method to generate $^1O_2$ selectively and efficiently through copper-based Fenton chemistry under circumneutral conditions enhanced by chloride as co-catalyst, with reactivity completely different than that observed in classical iron-based Fenton

chemistry. The mechanism of its formation was elucidated through the kinetic studies of orthogonally reactive reporter molecules, i.e., singlet oxygen sensor green, 4-hydroxy-2,2,6,6-tetramethylpiperidine, and phenol, and selective ROS quenchers. This method selectively generates $^1O_2$ *in situ* neither relying on photosensitization nor resulting in side reactions, and together with the mechanistic understanding of the Cu-Fenton reaction, not only opens new possibilities in many industries, such as organic synthesis and antimicrobial treatments, but also provides insight into Cu and H_2O_2 containing chemical, environmental, and biological systems.

Singlet oxygen ($^1O_2$), the first excited state of molecular oxygen, has been widely applied in various industries, e.g., serving as a synthetic reagent in chemical engineering,[1] an efficient disinfectant for combating microbial infection,[2] and an effective therapeutic for anticancer photodynamic therapy (PDT).[3] In addition, $^1O_2$ is involved in various biochemical processes, such as photosynthesis,[4] gene mutation,[5] phagocytosis,[6] cellular signalling,[7] and environmental degradation of natural organic matter.[8,9] As an important reactive oxygen species (ROS),[10,11] the high reactivity of $^1O_2$ results from its increased energy, i.e., with excitation energy of 94 kJ mol^{-1} relative to the ground state, and its extended lifetime, persisting >1 h in the gas phase, ~3.5 μs in water, ~3.0 μs in living cells, and ~31 ms in CCl_4,[12] a commonly used solvent in $^1O_2$-based organic synthesis. Efficient and facile generation of $^1O_2$ would greatly facilitate the application of its unique and selective reactivity in chemical and biological systems, which is currently not easily obtainable.

Although $^1O_2$ is ubiquitous in nature, chemical approaches to produce $^1O_2$ are limited. Currently, the most established method is through photosensitization of ground state oxygen via energy transfer from excited photosensitizer molecules,[1,13,14] semiconductors,[3,15] or noble metal nanoparticles.[16,17] However, this technique relies on the availability of both dissolved oxygen and light penetration, which are also limiting factors in PDT.[3] Thermal decomposition of endoperoxides,[18] dioxetanes and dioxiranes,[19] or perchromate,[20] and catalytic decomposition of peroxomonosulfate by $LaMnO_3$ perovskites[21] have been employed to generate $^1O_2$, but the starting materials are not commonly available or are toxic and are thus unsuitable for industrial use. Khan and Kasha discovered that the simple chemical reaction between hypochlorite ions and hydrogen peroxide (H_2O_2),[22,23] or acidification of hypochlorite,[24] was capable of producing $^1O_2$ in aqueous solutions, which offered the possibility of generating $^1O_2$ for both fundamental and applied research. However, the presence of hypochlorite in reaction media can result in unwanted chlorination of substrates, and this reaction is fairly rapid and not easily controlled. Herein we describe an alternate catalytic decomposition of H_2O_2 to form $^1O_2$ with high selectivity through the application of Cu-based Fenton chemistry at circumneutral pH. In this reaction the presence of Cl^- acts as a co-catalyst, greatly increasing the $^1O_2$ generation rate, but avoids the production of chlorinating species, resulting in selective reactivity. This greatly facilitates the use of chemically generated $^1O_2$ for chemical and biological applications and uncovers previously unknown details of Cu-based Fenton chemistry.

Fenton chemistry, the decomposition of H_2O_2 catalyzed by Fe^{2+} or Fe^{3+} ions under acidic conditions, has been widely studied since it was first discovered in 1894,[25] and is a reliable way of generating ROS that has major applications in advanced oxidation process-based water treatment[26] and has also been implicated in various physiological processes in biological systems.[27] Despite the controversy on the mechanisms of Fenton chemistry over the decades, it has been established with evidence that $^{\bullet}OH$ radicals and/or high valent Fe (Fe^{4+}=O) are the main ROS in the Fe-Fenton reaction. Similarly, $^{\bullet}OH$ and Cu^{3+} have been assumed to be the main ROS in Cu-Fenton chemistry.

In contrast, we found $^1O_2$ is the main ROS generated in the Cu-Fenton reaction, which is completely different than the classical Fe-based Fenton reaction, as demonstrated using orthogonally reactive reporter molecules and selective ROS quenchers. First, $^1O_2$ presence was monitored using singlet oxygen sensor green (SOSG), which is oxidized by $^1O_2$ in a highly selective manner to form an endoperoxide, which is a fluorescent product suitable for quantification (Fig. 1a and Supplementary Fig. 1a).[28,29] Furthermore, strong signals of TEMPO-OH, which is the oxidized product of TEMP-OH by $^1O_2$, was detected by an electron paramagnetic resonance (EPR) spectrometer (Supplementary Fig. 2);[30] however, this signal was quenched in the presence of azide, a known quencher of $^1O_2$, supporting the production of $^1O_2$ in the system.

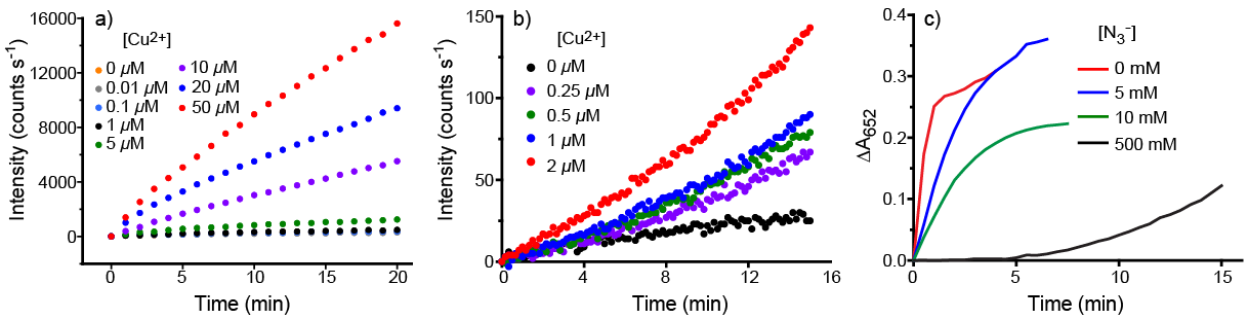

Figure 1. Oxidation rate of a) singlet oxygen sensor green (SOSG) and b) coumarin as a function of Cu^{2+} concentration, and c) quenching of 3,3',5,5'-tetramethylbenzidine (TMB) oxidation by various concentrations of NaN_3, a $^1O_2$ quencher. [SOSG] and [coumarin] = 100 μM, and [H_2O_2] = 500 mM; for c) [TMB] = 500 μM, [$CuCl_2$] = 1 μM, [NaCl] and [H_2O_2] = 500 mM.

A small amount of hydroxyl radical (•OH) production was observed by using the selective probe, coumarin, which forms a fluorescent product, umbelliferone, after reacting with •OH (Fig. 1b and Supplementary Fig. 1b).[31] However, •OH was ruled out as the main ROS in the Cu-Fenton reaction based on the following experiments. A chromogenic substrate, 3,3',5,5'-tetramethylbenzidine (TMB), was implemented as a nonselective indicator for the total ROS production because of its facile oxidation by many ROS except H_2O_2 ($E°$(ox-TMB/TMB) = 0.27 V). To demonstrate that $^1O_2$ is the main ROS, we tested the TMB oxidation in the presence of established selective ROS scavengers, including *t*-butyl alcohol (TBA) and coumarin, which quench •OH, and azide, which quenches $^1O_2$. The results (Supplementary Figs. 2–4) show that TMB

oxidation was unaffected by either ·OH scavenger, which is consistent with previous results, indicating that oxidation by ·OH did not contribute significantly to TMB oxidation, and thus ·OH was not generated in significant quantities.[32–36] However, TMB oxidation was quenched by excess azide in a dosage-dependent manner (Fig. 1c and Supplementary Fig. 1c), while it resumes after ~5 min when the azide is completely consumed. The recovery of TMB oxidation after the azide is consumed eliminates the possibility that azide is a simple catalyst poison but is rather competing with TMB for $^1O_2$ generated in the system. Altogether, this suggests that $^1O_2$, rather than ·OH, is the main ROS responsible for TMB oxidation. To further corroborate the conclusion, the TMB oxidation experiments were performed in deuterated water (80% D_2O). The lifetime of $^1O_2$ in D_2O is longer than that in H_2O, so oxidation of TMB and SOSG (75% D_2O) would be enhanced if $^1O_2$ was the main oxidant, because extending the excited state lifetime of $^1O_2$ increases the probability of it successfully reacting with an indicator molecule before relaxing to the ground state. This hypothesis was validated (Fig. 2a and Supplementary Figs. 5a and 6b), because both reactions were similarly enhanced. Taken together, the results reinforce $^1O_2$ as the major ROS in Cu-Fenton reaction.

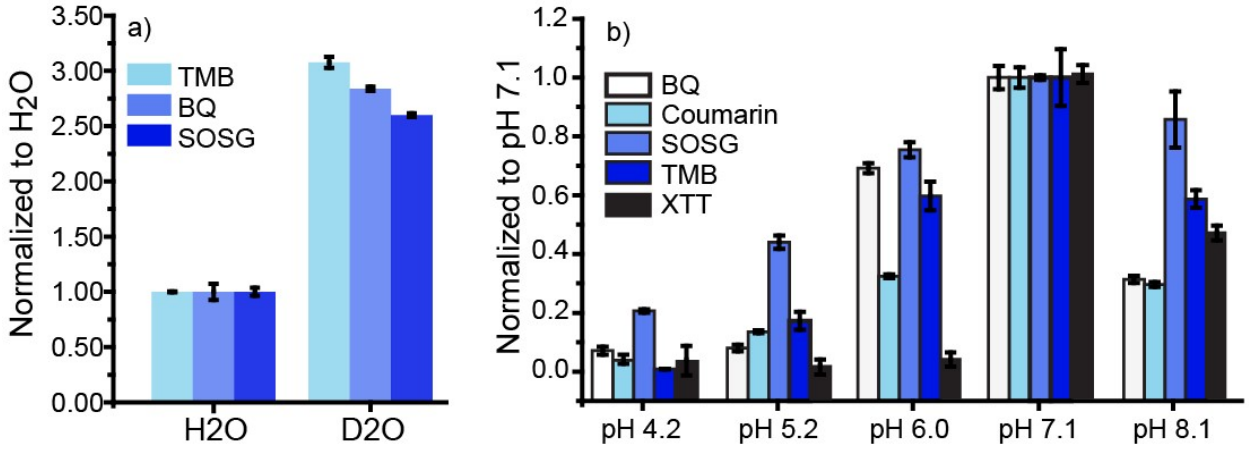

Figure 2. Normalized reaction rates of 3,3',5,5'-tetramethylbenzidine (TMB), singlet oxygen sensor green (SOSG), and coumarin oxidation and p-benzoquinone (BQ) formation as a function of a) solvent composition and b) pH. [buffer] = 1 mM, pH 4–6 MES and pH 7–8 MOPS. For TMB, SOSG, coumarin, and XTT: [TMB] = 500 μM, [SOSG] and [coumarin] = 100 μM, [XTT] = 1 mM, [$CuCl_2$] = 1 μM, and [NaCl] and [H_2O_2] = 500 mM. For phenol (PhOH): [PhOH] = 1 mM, [$CuCl_2$] = 50 μM, [NaCl] = 100 mM, and [H_2O_2] = 10 mM (Absolute rates in Supplementary Fig. 5). Error bars correspond to the standard error of the linear regression.

Furthermore, Cl^- dramatically accelerated the generation of $^1O_2$ production by the Cu-Fenton reaction, making it more efficient, as evidenced by acceleration of the oxidation of SOSG and TMB in the presence of Cl^- (Fig. 3). $^1O_2$ was found to be the only major ROS according to similar experimental evidence, including oxidation of TMB and SOSG being accelerated in 80% D_2O (Fig. 2a), and quenched by azide (Fig. 1c), but not by $^{\bullet}OH$ scavengers, such as TBA or coumarin (Supplementary Fig. 3).

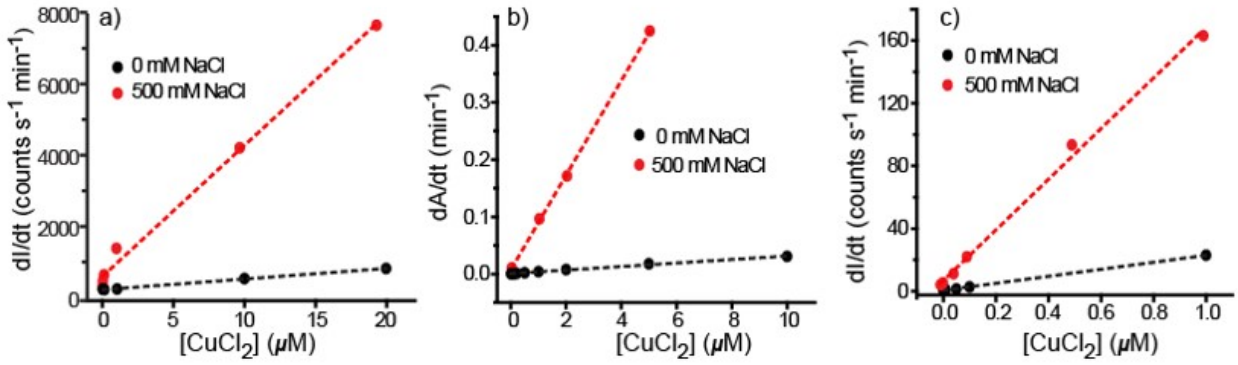

Figure 3. Oxidation rate enhancement of a) singlet oxygen sensor green (SOSG), b) 3,3',5,5'-tetramethylbenzidine (TMB) and c) coumarin by NaCl. [SOSG] and [coumarin] = 100 μM, [TMB] = 500 μM, and [H_2O_2] = 500 mM.

Previously chlorine radicals ($Cl^{\bullet}$ and $Cl_2^{-\bullet}$) were assumed the main reactive species based on observed chlorination of organic molecules under forcing conditions, i.e., in high [Cu^{2+}] and [Cl^-] systems under pH 4; however, under circumneutral pH conditions and low [Cu^{2+}], chlorinated products were not detected in the present experiments. Even if a small number of chlorine radicals are generated, they are not the main reactive species in the system and are unlikely to chlorinate substrates because they will react with the excess amount of H_2O_2 to form $^{\bullet}OH$ and $^1O_2$.[22–24] In addition to small amounts of $^{\bullet}OH$, a small amount of superoxide radicals ($O_2^{\bullet-}$) were detected in the system through reaction with the chromogenic XTT dye (Supplementary Fig. 7),[37] which is reduced by $O_2^{\bullet-}$, but is present at concentrations far less than the $^1O_2$ generated.

The selective generation of $^1O_2$ is highly useful. As demonstrated in our previous work, $^1O_2$ was used either for ultrasensitive colorimetric detection of Cu ions in water samples[33] or for antibacterial or anti-biofilm applications.[38] Importantly, as a selective oxidant and electrophile, it has been widely employed for organic synthesis, such as Diels-Alder 2+2 and 2+4 cycloadditions and ene-like reactions.[1,13,39–42] Herein, we demonstrate its application for selective synthesis of 1,4-benzoquinone (BQ) directly from phenol (PhOH), serving as a simple model of the selective oxidation of phenolic compounds, important intermediates for the pharmaceutical industry. Under synthetically relevant conditions ([H_2O_2] ≥100 mM) the reaction is complete within several seconds. The product can be extracted for GC-MS analysis, whereas the catalyst species (Cu and Cl^-) remain in the aqueous phase and can be used for subsequent reactions. The selectivity is up to 99% (45% yield, Supplementary Table 1) and no additional purification steps were needed. In addition, the yield of BQ was affected by pH, the concentrations of the reagents including H_2O_2, Cu, Cl^-, and the use of D_2O as solvent, in the same way as the oxidation of TMB and SOSG (Fig. 2 and Supplementary Figs. 8 and 9), which in combination with its remarkable selectivity (Supplementary Fig. 10),[14] further substantiates the role of $^1O_2$ as the main oxidant. Thus, Cu-Fenton chemistry, especially Cl^--accelerated Cu-Fenton chemistry, is a promising synthetic tool for the exploitation of the unique reactivity of $^1O_2$ in a cost-effective and simple manner with reduced unwanted reactivity and simple product purification.

Mechanistic understanding

In the Cu-Fenton system either in the presence or absence of chloride, our work established that $^1O_2$ is the main ROS, although a small amount of •OH and $O_2^{\bullet-}$ are always detected. The response of all three ROS to changes in pH or [Cl^-] follows the same pattern (Figs. 2b and 3 and Supplementary Figs. 5 and 7), indicating that they may be generated sequentially rather than simultaneously. Herein, $^{\bullet}OH$ and $O_2^{\bullet-}$ serve as intermediates in the catalytic cycle, being continuously consumed whenever generated. Consequently, $^{\bullet}OH$ and $O_2^{\bullet-}$ are detectable only at low static concentrations in the system (they occasionally escape the catalytic cycle, as detectable through reaction with coumarin or XTT, respectively), while $^1O_2$ leaves the cycle as an end product. Chlorination was occasionally detected in the system,[33,38] but only at lower pH values with high concentrations of Cu and Cl^- in a manner different from the other three ROS; thus, $Cl^{\bullet}$ is not considered an intermediate. A mechanism governing $^1O_2$ generation within the catalytic cycle is proposed in Fig. 4, which not only aligns with all established knowledge,[43] but also rationalizes all experimental observations.

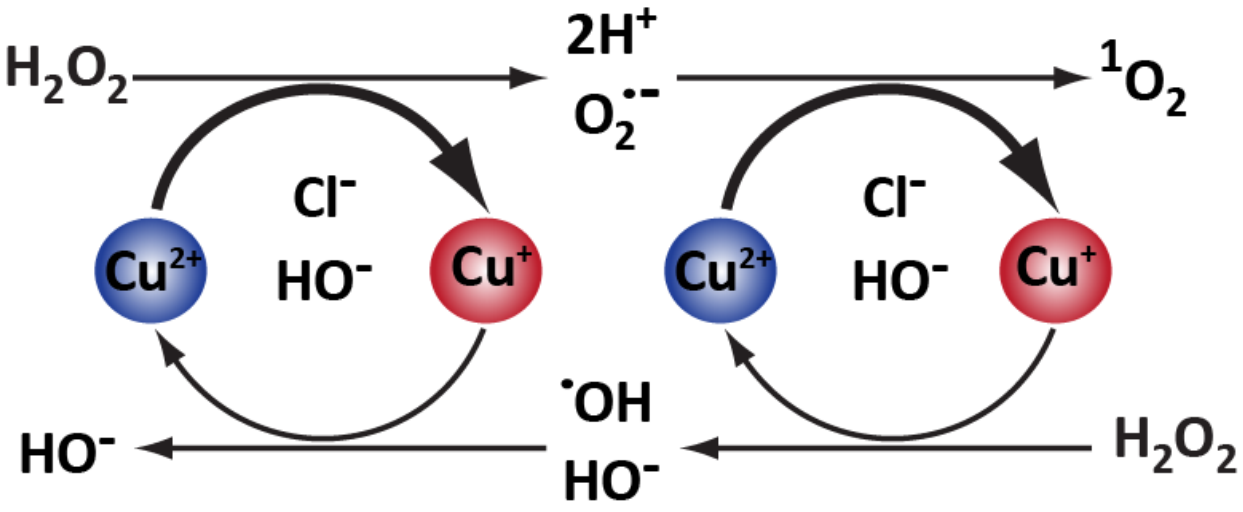

Figure 4. Mechanism of the generation of singlet oxygen in the copper-based Fenton reaction

First, $^1O_2$ is generated via two single electron oxidation steps from HO_2^- (deprotonation of H_2O_2 is very fast) by Cu^{2+}, where $O_2^{\bullet-}$ is an intermediate (equations (1) and (2)).

$$Cu^{2+} + HO_2^- \rightleftarrows Cu^+ + O_2^{\bullet-} + H^+ \quad (1)$$

$$Cu^{2+} + O_2^{\bullet-} \rightleftarrows Cu^+ + {}^1O_2 \quad (2)$$

Because $^1O_2$ production is first-order with respect to [Cu] and [H_2O_2] (Supplementary Fig. 9), it suggests that the rate determining step is oxidation of either H_2O_2 (equation (1)) or $O_2^{\bullet-}$ (equation (2)). Based on literature, equation (1) is a slower process than equation (2),[43] thus being the rate-determining step in the overall cycling. In the Cl^--Cu-Fenton reaction, the H_2O_2 oxidation reaction is also first-order in respect to [Cl^-]

(Supplementary Fig. 9), where it presumably serves as a co-catalyst that facilitates the reduction of Cu^{2+} in the first two steps (equations (1) and (2)) by forming a $CuCl^{+}$ complex, as demonstrated previously (importantly the rate is not zero when $[Cl^{-}] = 0$, Supplementary Fig. 9a, indicating that the regular Cu-Fenton reaction without chloride also generates the same ROS).[32,43,44] The effects of other halides and cations on TMB oxidation were previously explored.[33] Similar to chloride, the hydroxide ion concentration (pOH) affects the oxidation of H_2O_2, presumably by facilitating the deprotonation of H_2O_2 to form HO_2^{-}, a better electron donor for Cu^{2+} (Fig. 2b). In addition, together with Cl^{-}, OH^{-} affects the speciation of Cu^{2+} by forming more strongly oxidative complexes, such as CuClOH.[32,43,44]

To complete the redox cycling of Cu^{+}/Cu^{2+}, Cu^{+} is re-oxidized by successive single electron transfers to H_2O_2 and the intermediate oxidant, $^{\bullet}OH$ (equations (3) and (4)).

$$Cu^{+} + H_2O_2 \rightleftarrows Cu^{2+} + HO^{\bullet} + HO^{-} \quad (3)$$

$$Cu^{+} + HO^{\bullet} \rightleftarrows Cu^{2+} + HO^{-} \quad (4)$$

The overall reaction described by equations (1)–(4) is the conversion of two H_2O_2 molecules to two H_2O molecules and one $^1O_2$. Based on previous work,[43,44] oxidation of Cu^{+} is not rate limiting, although Cl^{-} may inhibit the Cu^{+} oxidation by ~60%. However, the degree of acceleration of Cu^{2+} reduction increases dramatically, i.e., ~10^8 times;[43] therefore, the overall turnover frequency of the Cu-Fenton reaction is increased, which

results in highly efficient $^1O_2$ generation. In addition, because the H_2O_2 concentrations in our system is much higher (mM level) than dissolved oxygen (μM level), the effect of the latter is negligible.

In our system, either with or without chloride, the level of the intermediate radicals, $HO^{\bullet}$ and $O_2^{\bullet-}$, remains low throughout the reaction period. When $HO^{\bullet}$ and $O_2^{\bullet-}$ escape the catalytic cycle by reacting with scavengers, such as coumarin and XTT, there might be a mechanism by which [$HO^{\bullet}$] and [$O_2^{\bullet-}$] maintain balance to prevent buildup of these radicals in the system, which would otherwise be significant. As the reaction medium contains [H_2O_2] $\gg$ [$HO^{\bullet}$] and [$O_2^{\bullet-}$], these radicals can react with H_2O_2 to form the opposite radical and H^+ and H_2O or $^1O_2$ and ^{-}OH, respectively (equations (5) and (6)).

$$O_2^{-\cdot} + H_2O_2 \rightleftarrows {}^1O_2 + {}^{\cdot}OH + {}^{-}OH \quad (5)$$

$$^{\cdot}OH + H_2O_2 \rightleftarrows H_2O + O_2^{-\cdot} + H^+ \quad (6)$$

These reactions are slow compared to the Cu-catalyzed reactions but serve to prevent accumulation of one radical over the other during reaction initiation, or as radicals are scavenged outside of the catalytic cycle.

In brief, the chloride accelerated Cu-Fenton reaction not only offers a simple and cost-effective approach for selective generation of $^1O_2$, greatly facilitating its application in chemical synthesis, antimicrobial treatments, and spectroscopic applications, but also

reveals important new insight into the ubiquitous Cu-containing systems when H_2O_2 is present or generated, e.g., by environmental photochemistry, chemical industry, or biological metabolism, and thus has potential for applications and implications in many areas, such as immunology, aging, and oxidative-stress related degenerative diseases.

Acknowledgements

This work was supported by the Atlantic Canada Opportunities Agency AIF program, Nova Scotia Lands Boat Harbour Remediation Program, Cape Breton University RISE program, NSERC Discovery Grants Program, Beatrice Hunter Cancer Research Institute (BHCRI), and Guangdong Province Higher Vocational College & School's Pearl River Scholar Funded Scheme (2017).

Author contributions

A.J.C., S.L.M., and X.Z. designed the experiments; A.J.C., D.O., and C. N. performed experimental research; A.J.C., Y.C., K.O, S.L.M., and X.Z. wrote the manuscript.

Completing Interest Statement

The authors declare no competing interests.

References

1. Ghogare, A. A. & Greer, A. Using Singlet Oxygen to Synthesize Natural Products and Drugs. *Chem. Rev.* **116,** 9994–10034 (2016).
2. Kammerlander, G. *et al.* A clinical evaluation of the efficacy and safety of singlet oxygen in cleansing and disinfecting stagnating wounds. *J. Wound Care* **20,** 149–150, 152, 154 passim (2011).
3. Samia, A. C. S., Chen, X. & Burda, C. Semiconductor Quantum Dots for Photodynamic Therapy. *J. Am. Chem. Soc.* **125,** 15736–15737 (2003).
4. Triantaphylidès, C. & Havaux, M. Singlet oxygen in plants: production, detoxification and signaling. *Trends Plant Sci.* **14,** 219–228 (2009).
5. Agnez-Lima, L. F., Mascio, P. D., Napolitano, R. L., Fuchs, R. P. & Menck, C. F. M. Mutation Spectrum Induced by Singlet Oxygen in Escherichia coli Deficient in Exonuclease III. *Photochem. Photobiol.* **70,** 505–511 (1999).
6. Allen, R. C. Role of oxygen in phagocyte microbicidal action. *Environ. Health Perspect.* **102,** 201–208 (1994).
7. Mittler, R. *et al.* ROS signaling: the new wave? *Trends Plant Sci.* **16,** 300–309 (2011).

8. Niu, X.-Z., Busetti, F., Langsa, M. & Croué, J.-P. Roles of singlet oxygen and dissolved organic matter in self-sensitized photo-oxidation of antibiotic norfloxacin under sunlight irradiation. *Water Res.* **106,** 214–222 (2016).
9. Haag, W. R., Hoigné, J., Gassman, E. & Braun, A. Singlet oxygen in surface waters — Part I: Furfuryl alcohol as a trapping agent. *Chemosphere* **13,** 631–640 (1984).
10. Ogilby, P. R. Singlet oxygen: there is indeed something new under the sun. *Chem. Soc. Rev.* **39,** 3181–3209 (2010).
11. Bodesheim, M. & Schmidt, R. Chemical Reactivity of Sigma Singlet Oxygen O2(1Σg+). *J. Phys. Chem. A* **101,** 5672–5677 (1997).
12. Jenny, T. A. & Turro, N. J. Solvent and deuterium isotope effects on the lifetime of singlet oxygen determined by direct emission spectroscopy at 1.27 μm. *Tetrahedron Lett.* **23,** 2923–2926 (1982).
13. Schenck, G. O. Zur Theorie der photosensibilisierten Reaktion mit molekularem Sauerstoff. *Naturwissenschaften* **35,** 28–29 (1948).
14. Li, C. & Hoffman, M. Z. Oxidation of Phenol by Singlet Oxygen Photosensitized by the Tris(2,2'-bipyridine)ruthenium(II) Ion. *J. Phys. Chem. A* **104,** 5998–6002 (2000).
15. Xiao, L., Gu, L., Howell, S. B. & Sailor, M. J. Porous Silicon Nanoparticle Photosensitizers for Singlet Oxygen and Their Phototoxicity against Cancer Cells. *ACS Nano* **5,** 3651–3659 (2011).
16. Long, R. *et al.* Surface Facet of Palladium Nanocrystals: A Key Parameter to the Activation of Molecular Oxygen for Organic Catalysis and Cancer Treatment. *J. Am. Chem. Soc.* **135,** 3200–3207 (2013).

17. Vankayala, R., Sagadevan, A., Vijayaraghavan, P., Kuo, C.-L. & Hwang, K. C. Metal nanoparticles sensitize the formation of singlet oxygen. *Angew. Chem. Int. Ed Engl.* **50,** 10640–10644 (2011).
18. Aubry, J.-M., Pierlot, C., Rigaudy, J. & Schmidt, R. Reversible Binding of Oxygen to Aromatic Compounds. *Acc. Chem. Res.* **36,** 668–675 (2003).
19. Adam, W., Kazakov, D. V. & Kazakov, V. P. Singlet-Oxygen Chemiluminescence in Peroxide Reactions. *Chem. Rev.* **105,** 3371–3387 (2005).
20. Peters, J. W., Pitts, J. N., Rosenthal, I. & Fuhr, H. New and unique chemical source of singlet molecular oxygen. Potassium perchromate. *J. Am. Chem. Soc.* **94,** 4348–4350 (1972).
21. Tian, X. *et al.* A novel singlet oxygen involved peroxymonosulfate activation mechanism for degradation of ofloxacin and phenol in water. *Chem. Commun.* **53,** 6589–6592 (2017).
22. Khan, A. U. & Kasha, M. Red Chemiluminescence of Molecular Oxygen in Aqueous Solution. *J. Chem. Phys.* **39,** 2105–2106 (1963).
23. Seliger, H. H. Chemiluminescence of H2O2–NaOCl Solutions. *J. Chem. Phys.* **40,** 3133–3134 (1964).
24. Khan, A. U. & Kasha, M. Singlet molecular oxygen evolution upon simple acidification of aqueous hypochlorite: application to studies on the deleterious health effects of chlorinated drinking water. *Proc. Natl. Acad. Sci.* **91,** 12362–12364 (1994).
25. Fenton, H. J. H. LXXIII.—Oxidation of tartaric acid in presence of iron. *J. Chem. Soc. Trans.* **65,** 899–910 (1894).

26. Oturan, M. A. & Aaron, J.-J. Advanced Oxidation Processes in Water/Wastewater Treatment: Principles and Applications. A Review. *Crit. Rev. Environ. Sci. Technol.* **44,** 2577–2641 (2014).
27. Prousek, J. Fenton chemistry in biology and medicine. *Pure Appl. Chem.* **79,** 2325–2338 (2007).
28. Santaella, C. *et al.* Aged TiO2-Based Nanocomposite Used in Sunscreens Produces Singlet Oxygen under Long-Wave UV and Sensitizes Escherichia coli to Cadmium. *Environ. Sci. Technol.* **48,** 5245–5253 (2014).
29. Dimitrijevic, N. M., Rozhkova, E. & Rajh, T. Dynamics of Localized Charges in Dopamine-Modified TiO2 and their Effect on the Formation of Reactive Oxygen Species. *J. Am. Chem. Soc.* **131,** 2893–2899 (2009).
30. Wang, H. *et al.* Ultrathin Black Phosphorus Nanosheets for Efficient Singlet Oxygen Generation. *J. Am. Chem. Soc.* **137,** 11376–11382 (2015).
31. Louit, G. *et al.* The reaction of coumarin with the OH radical revisited: hydroxylation product analysis determined by fluorescence and chromatography. *Christ. Ferradini Meml. Issue* **72,** 119–124 (2005).
32. Xing, G., Pham, A. N., Miller, C. J. & Waite, T. D. pH-dependence of production of oxidants (Cu(III) and/or HO•) by copper-catalyzed decomposition of hydrogen peroxide under conditions typical of natural saline waters. *Geochim. Cosmochim. Acta* **232,** 30–47 (2018).
33. Shan, Z. *et al.* Chloride accelerated Fenton chemistry for the ultrasensitive and selective colorimetric detection of copper. *Chem. Commun.* **52,** 2087–2090 (2016).

34. Pham, A. N., Xing, G., Miller, C. J. & Waite, T. D. Fenton-like copper redox chemistry revisited: Hydrogen peroxide and superoxide mediation of copper-catalyzed oxidant production. *J. Catal.* **301,** 54–64 (2013).
35. Feng, Y. *et al.* Degradation of contaminants by Cu+-activated molecular oxygen in aqueous solutions: Evidence for cupryl species (Cu3+). *J. Hazard. Mater.* **331,** 81–87 (2017).
36. Lee, H. *et al.* Chloride-enhanced oxidation of organic contaminants by Cu(II)-catalyzed Fenton-like reaction at neutral pH. *J. Hazard. Mater.* **344,** 1174–1180 (2018).
37. Li, Y., Zhang, W., Niu, J. & Chen, Y. Mechanism of Photogenerated Reactive Oxygen Species and Correlation with the Antibacterial Properties of Engineered Metal-Oxide Nanoparticles. *ACS Nano* **6,** 5164–5173 (2012).
38. Wang, L. *et al.* Chloride-accelerated Cu-Fenton chemistry for biofilm removal. *Chem. Commun.* **53,** 5862–5865 (2017).
39. Fritzsche, J. Ueber die festen Kohlenwasserstoffe des Steinkohlentheers. *Compt Rend Acad Sci Paris* **69,** 78 (1867).
40. Schenck, G. O. & Ziegler, K. Die Synthese des Ascaridols. *Naturwissenschaften* **32,** 157–157 (1944).
41. Wasserman, H. H. & Ives, J. L. Singlet oxygen in organic synthesis. *Tetrahedron* **37,** 1825–1852 (1981).
42. Frimer, A. A. The reaction of singlet oxygen with olefins: the question of mechanism. *Chem. Rev.* **79,** 359–387 (1979).

43. Moffett, J. W. & Zika, R. G. Reaction kinetics of hydrogen peroxide with copper and iron in seawater. *Environ. Sci. Technol.* **21,** 804–810 (1987).

44. Millero, F. J., Sharma, V. K. & Karn, B. The rate of reduction of copper(II) with hydrogen peroxide in seawater. *React. Chem. Species Aquat. Environ.* **36,** 71–83 (1991).

Supporting Information

Selective Generation of Singlet Oxygen in Chloride Accelerated Copper Fenton Chemistry

Andrew J. Carrier,[a] Collins Nganou,[a] David Oakley,[a] Yongli Chen,[b] Ken Oakes,[c] Stephanie L. MacQuarrie,[d] and Xu Zhang*[a]

[a]Veschuren Centre for Sustainability in Energy and the Environment, Cape Breton University, Sydney, Nova Scotia, B1P 6L2, Canada

[b]Postdoctoral Innovation Practice Base, Shenzhen Polytechnic, Shenzhen, 518055, China

[c]Department of Biology and [d]Department of Chemistry, Cape Breton University, Sydney, Nova Scotia, B1P 6L2, Canada

*Corresponding Author. E-mail: Xu_Zhang@cbu.ca

Experimental Details

Materials

Copper (II) chloride, sodium chloride, lithium chloride, sodium azide, t-butanol, phenol (PhOH), p-benzoquinone (BQ), 3,3',5,5'-tetramethylbenzidine (TMB), coumarin,

umbelliferone, 4-hydroxy-2,2,6,6-tetramethylpiperidine (TEMP-OH), 2,2,6,6-tetramethylpiperidine-N-oxyl (TEMPO), MOPS, MES, deuterium oxide, and dimethylsulfoxide (DMSO) were purchased from Sigma-Aldrich (Oakville, ON, Canada). Hydrogen peroxide (30 wt%, 9.77 M), methylene chloride, and methanol were purchased from Fisher Scientific (Ottawa, ON, Canada). Singlet oxygen sensor green (SOSG) was purchased from Thermo-Fisher (Waltham, MA, USA). XTT sodium salt was purchased from Alfa Aesar (Ward Hill, MA, USA). Nanopure water (18.2 MΩ cm) was obtained daily from a Barnstead Nanopure system (Thermo Scientific, Waltham, MA, USA). All reagents were used as received.

Equipment

UV-Vis absorbance and fluorescence data were obtained using a Tecan Infinite M1000 Pro microplate reader (Thermo-Fisher, Waltham, MA, USA). UV transparent Greiner 96-well flat bottom polystyrol microplates (Greiner, Kremsmünster, Austria) were used to measure oxidation of phenol, Costar 96-well flat bottom transparent polystyrol microplates (Corning, NY, USA) were used for TMB oxidation experiments, and Nunclon 96-well flat bottom black polystyrol plates (Thermo Fisher, Waltham, MA, USA) were used for fluorescence experiments. All reaction kinetics were measured at 25 ºC. Electron paramagnetic resonance (EPR) spectra were obtained using a Bruker microESR (Bruker, Billerica, MA, USA). Gas chromatography-mass spectrometry was performed using an Aglient Technologies 6890N gas chromatograph coupled with a 5973 Inert mass

spectrum detector (Santa Clara, CA, USA). An NSP-5 Inert capillary column (15 m x 0.25 mm x 0.30 μm, J&K Scientific, Edwardsville, NS, Canada) was used for the separation. The temperature program was initially 55 ºC for 4 min, then ramping at 15 ºC min^{-1} until reaching 130 ºC, then ramping at 20 ºC min^{-1} until reaching 260 ºC and holding for 7 min.

Phenol oxidation

All experiments were performed in microplates with final reaction volumes of 200 μL. The initial [PhOH] = 1 mM and [H_2O_2] = 10 mM to minimize the contribution to UV absorbance. $CuCl_2$, NaCl, and 1 mM of MES or MOPS buffer were added as appropriate to the experiment. The reactions were initiated by addition of H_2O_2. [PhOH] and [BQ] were monitored at their respective λ_{max} of 270 and 288 nm, with signal deconvolution based on calibration curves for both species at each wavelength as the solution of a system of two equations with two unknowns. PhOH and BQ are the only significant volatile small molecule species as determined by GC-MS, although there is formation of melanin-like polymerized BQ under these oxidation conditions.

TMB oxidation

All experiments were performed in microplates with final reaction volumes of 200 μL. Stock TMB solution was prepared in DMSO. The initial [TMB] = 500 μM, with [$CuCl_2$],

[NaCl], [H_2O_2], buffer, and D_2O being used as necessary. The reactive oxidant species quenchers t-BuOH, coumarin, and azide were added as necessary in separate experiments. The reaction was monitored at 652 nm, the λ_{max} of the oxidized TMB dimer charge transfer complex.

Coumarin oxidation

All experiments were performed in microplates with final reaction volumes of 200 μL. Stock coumarin solution was prepared in water. The initial [coumarin] = 100 μM, with [$CuCl_2$], [NaCl], [H_2O_2], and buffer being used as necessary. The reaction was monitored via fluorescence of the expected product of hydroxyl radical oxidation, umbelliferone, at excitation and emission wavelengths of 325 and 452 nm, respectively. In experiments using varying pH the relative fluorescence intensity of umbelliferone was corrected to that of pH 7 using fluorescence data obtained from commercially supplied umbelliferone at varying pH.

SOSG oxidation

All experiments were performed in microplates with final reaction volumes of 200 μL. Stock coumarin solution was prepared in methanol. The initial [SOSG] = 100 μM, with [$CuCl_2$], [NaCl], [H_2O_2], and buffer being used as necessary. The reaction was monitored

via fluorescence of the expected product of singlet oxygen oxidation, SOSG endoperoxide, at excitation and emission wavelengths of 504 and 525 nm, respectively.

TEMP-OH oxidation

TEMP-OH (100 μM) was prepared in water to which final concentrations of [$CuCl_2$], [NaCl], and [H_2O_2] of 1 μM, 500 mM, and 100 mM, respectively were added. The resultant solution was drawn into a capillary tube that was sealed at both ends. The capillary tube was then inserted into the EPR spectrometer to measure the EPR spectrum. This was comparable to the spectrum obtained from TEMPO.

XTT reduction

All experiments were performed in microplates with final reaction volumes of 200 μL. Stock XTT sodium salt solution was prepared in DMSO (10 mM). The initial [XTT] = 1 mM, with [$CuCl_2$], [NaCl], [H_2O_2], and buffer being used as necessary (with concentrations of 1 μM, 500 mM, and 500 mM, respectively unless otherwise stated). The reaction was monitored via absorbance of the expected product of superoxide radical anion reduction at 470 nm.

Supplemental Data

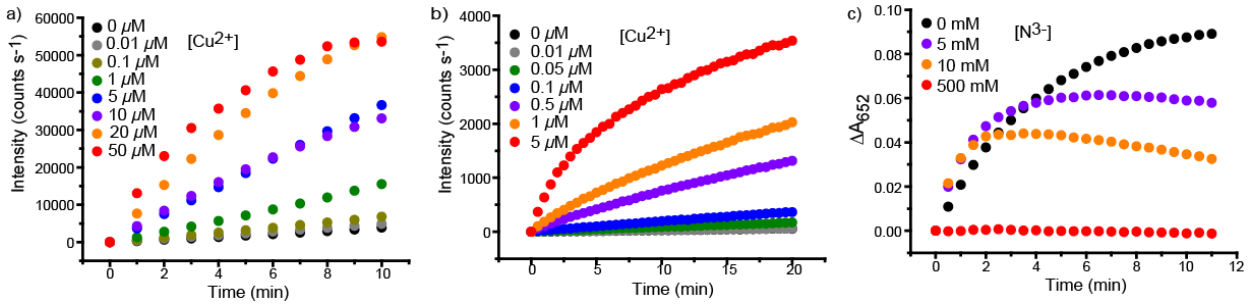

Figure S1. Oxidation rate of a) singlet oxygen sensor green (SOSG) and b) coumarin as a function of Cu^{2+} concentration, and c) quenching of 3,3',5,5'-tetramethylbenzidine (TMB) oxidation by various concentrations of NaN_3, a $^1O_2$ quencher. [SOSG] and [coumarin] = 100 μM, [H_2O_2] and [NaCl] = 500 mM; for b) [TMB] = 500 μM, [$CuCl_2$] = 1 μM, [NaCl] = 0 mM and [H_2O_2] = 500 mM.

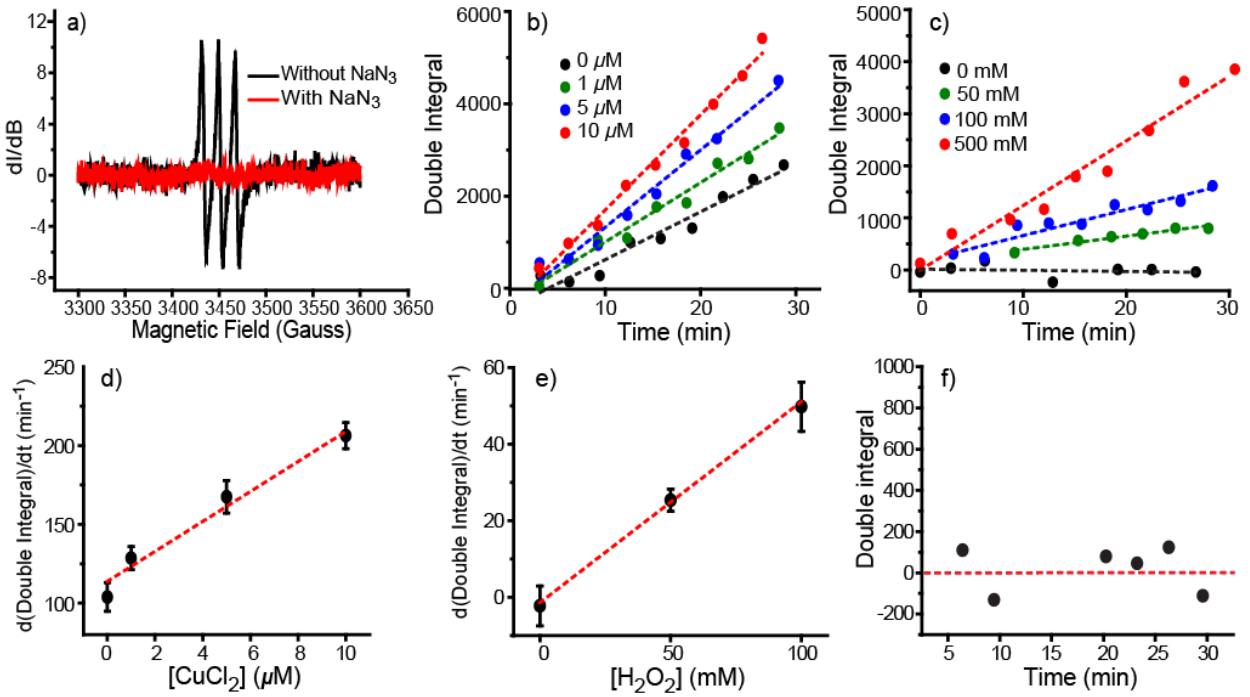

Figure S2. a) TEMPO-OH electron paramagnetic resonance (EPR) spectra formed in the presence and absence of added NaN_3. EPR signal intensity as a function of time formed from 50 mM of TEMP-OH with b) varying [$CuCl_2$] and 500 mM of NaCl and H_2O_2, c) and varying [H_2O_2] and 500 mM of NaCl and 1 μM $CuCl_2$; d) and e) are initial rate vs. varied quantity for b) and c), respectively; e) shows signal quenching by 500 mM NaN_3 ([$CuCl_2$] = 1 μM, and [NaCl] and [H_2O_2] = 500 mM) as a function of time.

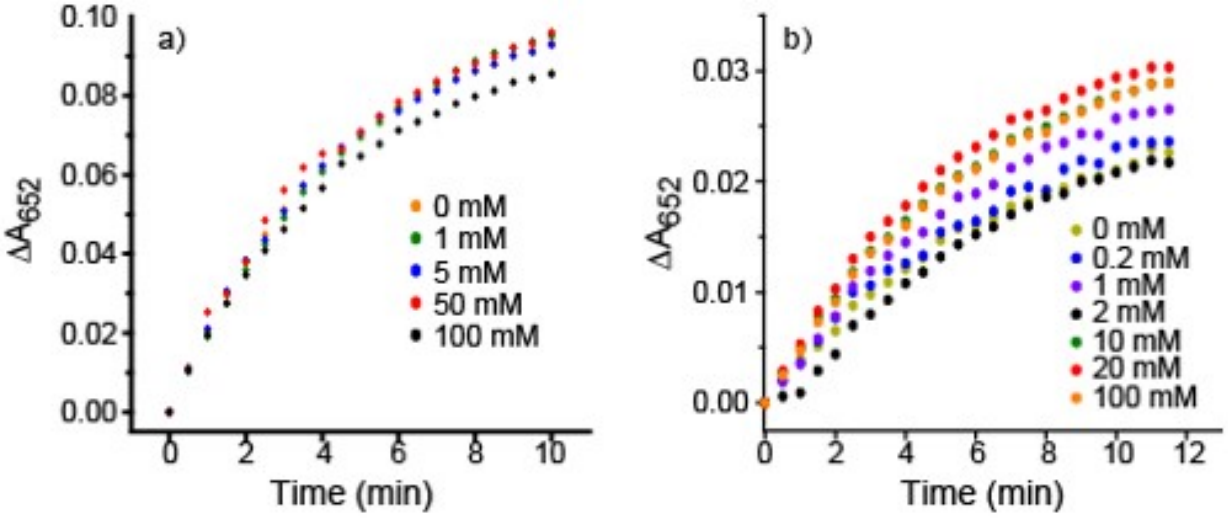

Figure S3. 3,3',5,5'-Tetramethylbenzidine (TMB) oxidation in the presence of increasing amounts of the ·OH scavengers a) t-butyl alcohol and b) coumarin. [TMB] = 500 μM, [$CuCl_2$] = 1 μM, [H_2O_2] and [NaCl] = 500 mM.

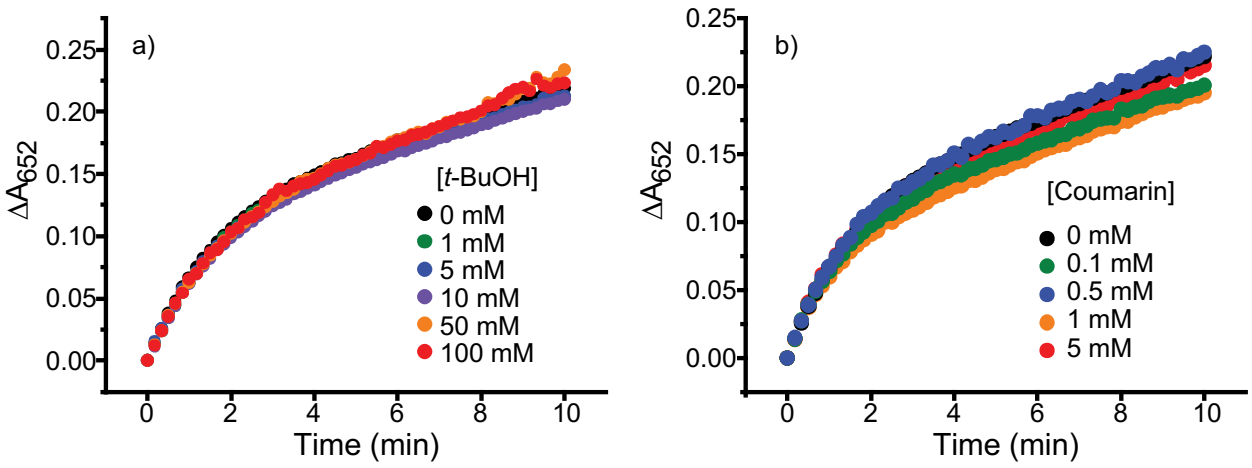

Figure S4. 3,3',5,5'-Tetramethylbenzidine (TMB) oxidation in the presence of increasing amounts of the ·OH scavengers a) t-butyl alcohol and b) coumarin. [TMB] = 500 μM, [$CuCl_2$] = 1 μM, [H_2O_2] = 500 mM and [NaCl] = 0 mM.

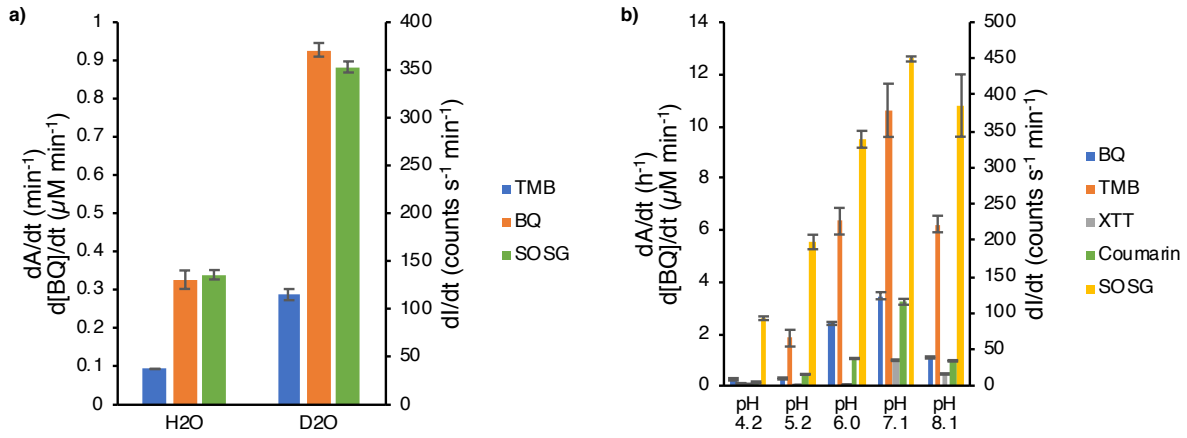

Figure S5. Reaction rates of 3,3',5,5'-tetramethylbenzidine (TMB), singlet oxygen sensor green (SOSG), and coumarin oxidation and p-benzoquinone (BQ) formation as a function of a) solvent composition and b) pH. [buffer] = 1 mM, pH 4–6 MES and pH 7–8 MOPS. For TMB, SOSG, coumarin, and XTT: [TMB] = 500 μM, [SOSG] and [coumarin] = 100 μM, [XTT] = 1 mM, [$CuCl_2$] = 1 μM, and [NaCl] and [H_2O_2] = 500 mM. For phenol (PhOH): [PhOH] = 1 mM, [$CuCl_2$] = 50 μM, [NaCl] = 100 mM, and [H_2O_2] = 10 mM.

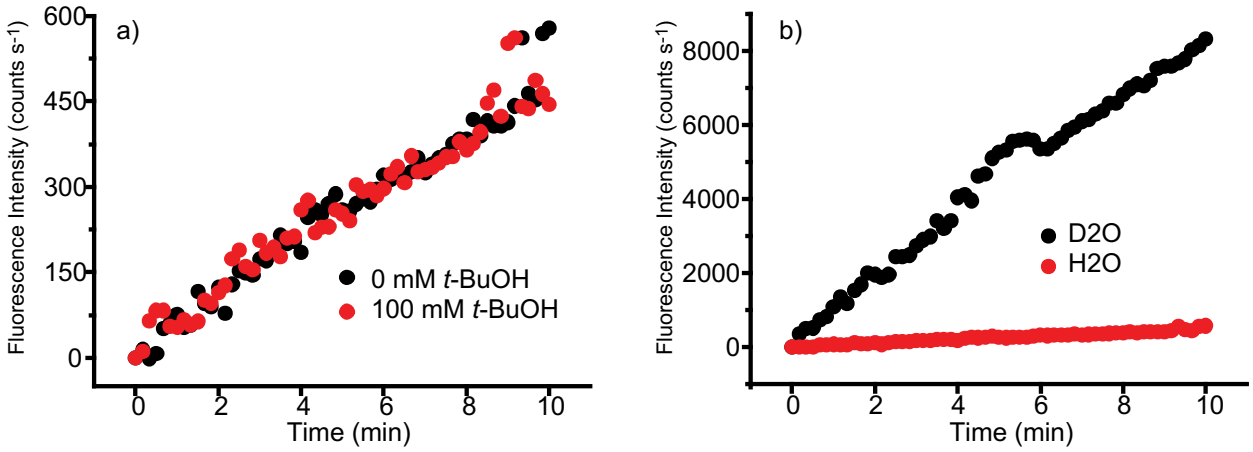

Figure S6. Singlet oxygen sensor green (SOSG) oxidation as a function of a) $^{\bullet}OH$ scavenging by t-butyl alcohol and b) solvent (H_2O vs 80% D_2O) in the absence of added NaCl.

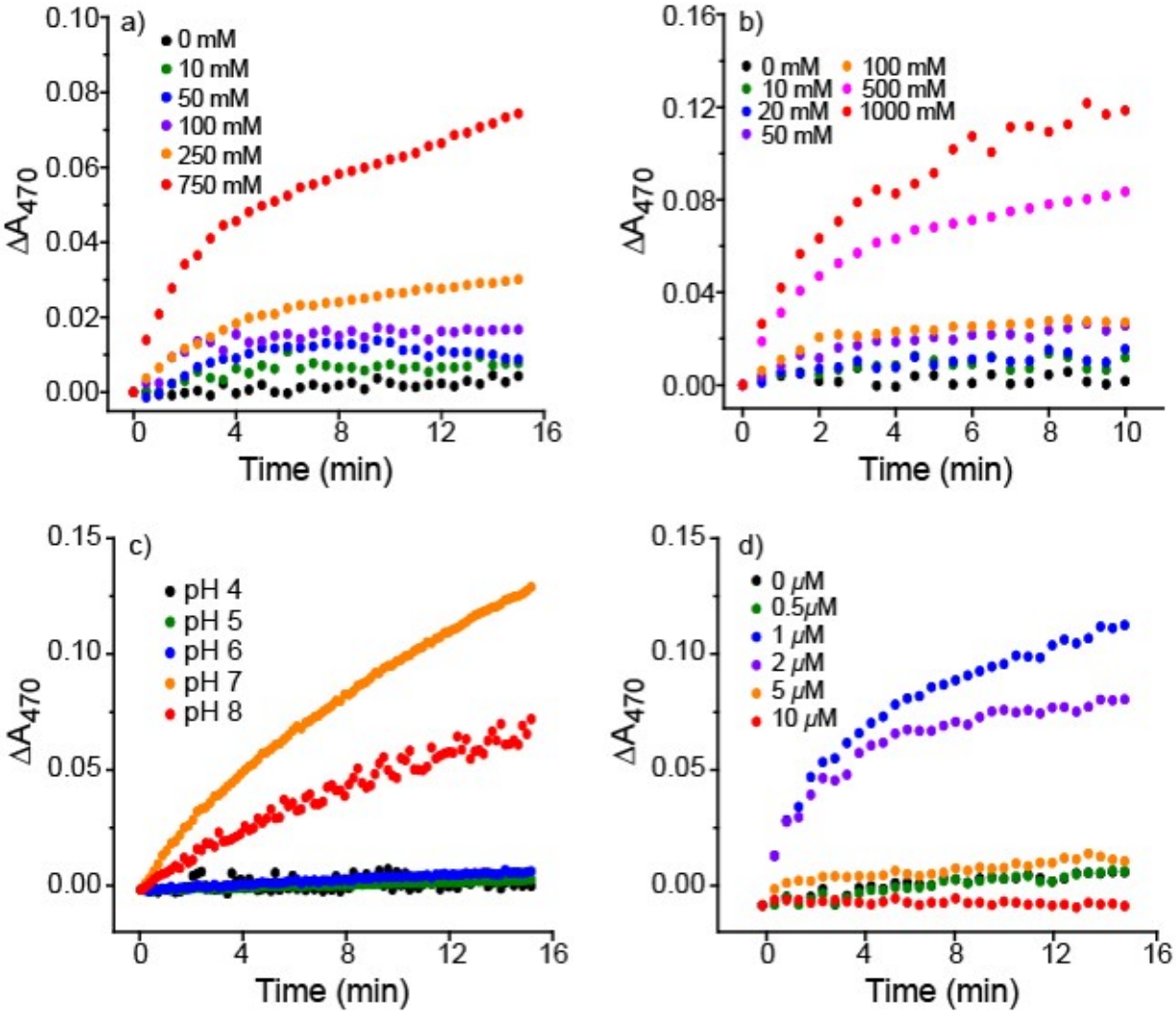

Figure S7. 2,3-bis-(2-methoxy-4-nitro-5-sulfophenyl)-2H-tetrazolium-5-carboxanilide (XTT) reduction as a function of a) varying NaCl, b) varying H_2O_2, c) varying pH, and d) varying $CuCl_2$. [XTT] and [MES buffer] = 1 mM; [NaCl] and [H_2O_2] = 500 mM and [$CuCl_2$] = 1 μM unless otherwise stated. Maximum rate observed when [$CuCl_2$] is 1–2 μM is reproducible and may be related to the rate of $O_2^{\cdot-}$ formation and its binding affinity to Cu^{2+}.

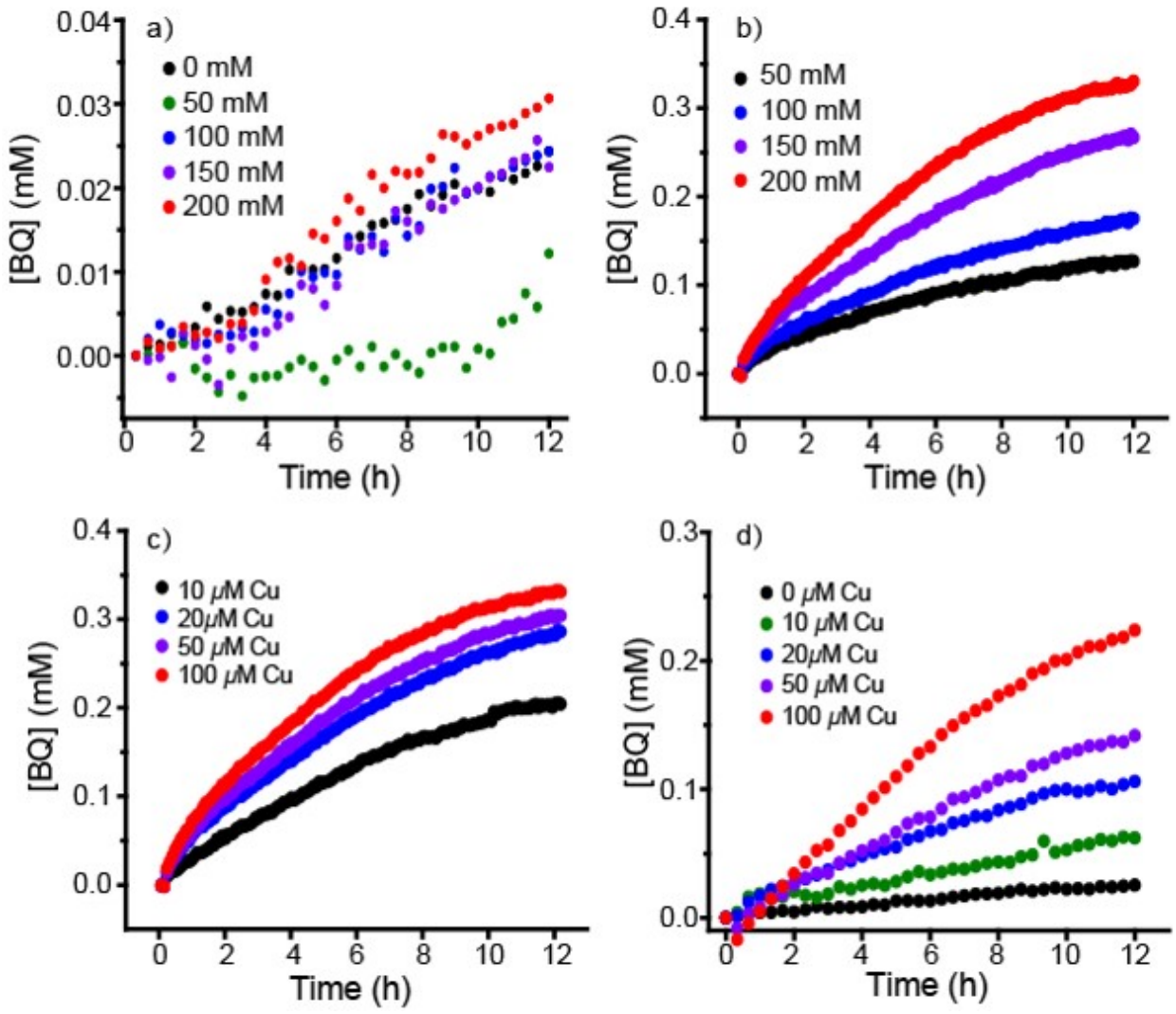

Figure S8. Phenol (PhOH) oxidation to form p-benzoquinone (BQ) with a) no $CuCl_2$ and varied NaCl, b) 50 μM $CuCl_2$ and varied NaCl, c) 100 mM NaCl and varied $CuCl_2$, and d) no NaCl and varied $CuCl_2$. [PhOH] = 1 mM and [H_2O_2] = 10 mM.

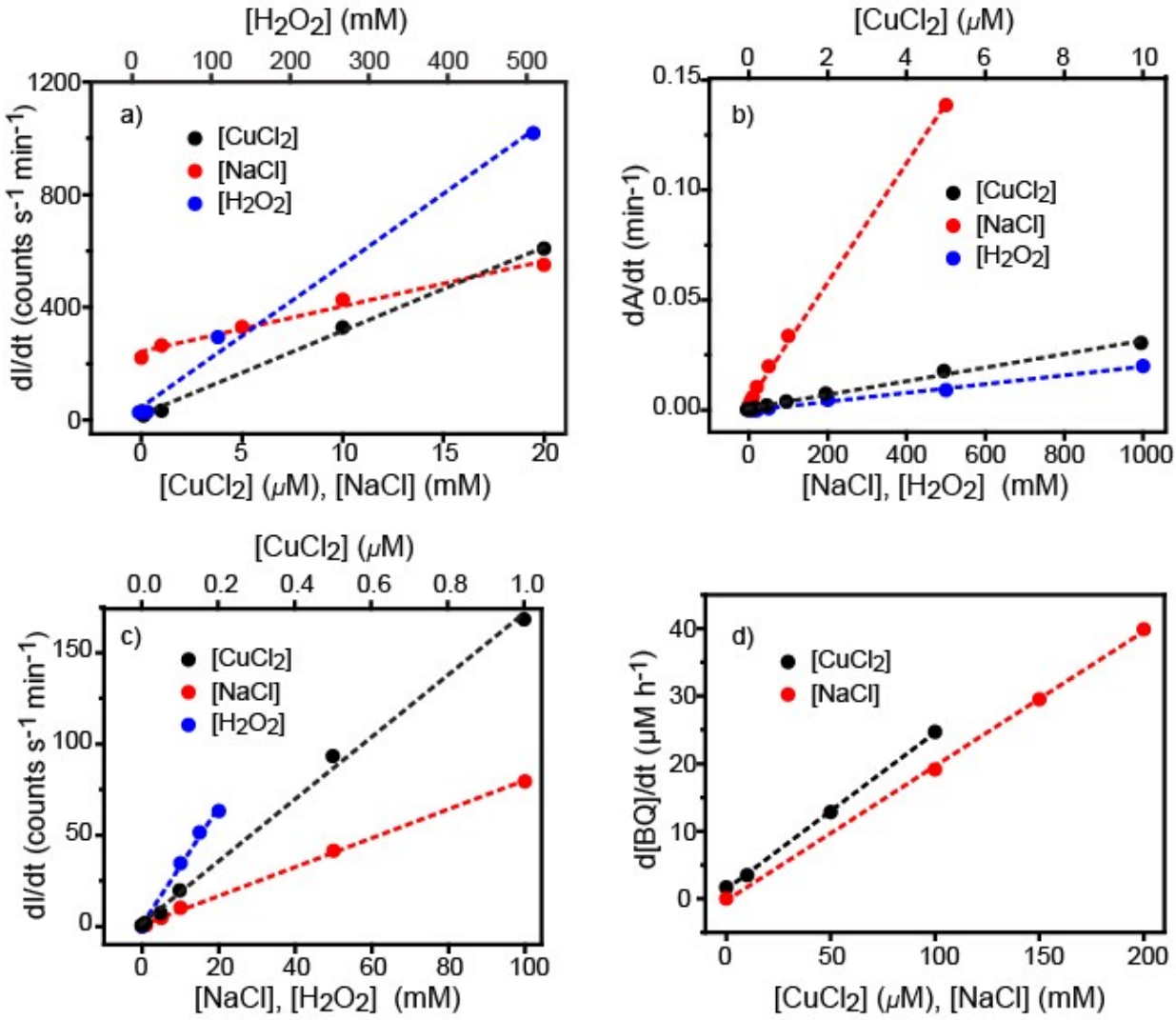

Figure S9. Initial reactions rates with varying initial $CuCl_2$, H_2O_2, and NaCl concentrations for a) singlet oxygen sensor green, b) coumarin, c) 3,3',5,5'-tetramethylbenzidine, and d) phenol.

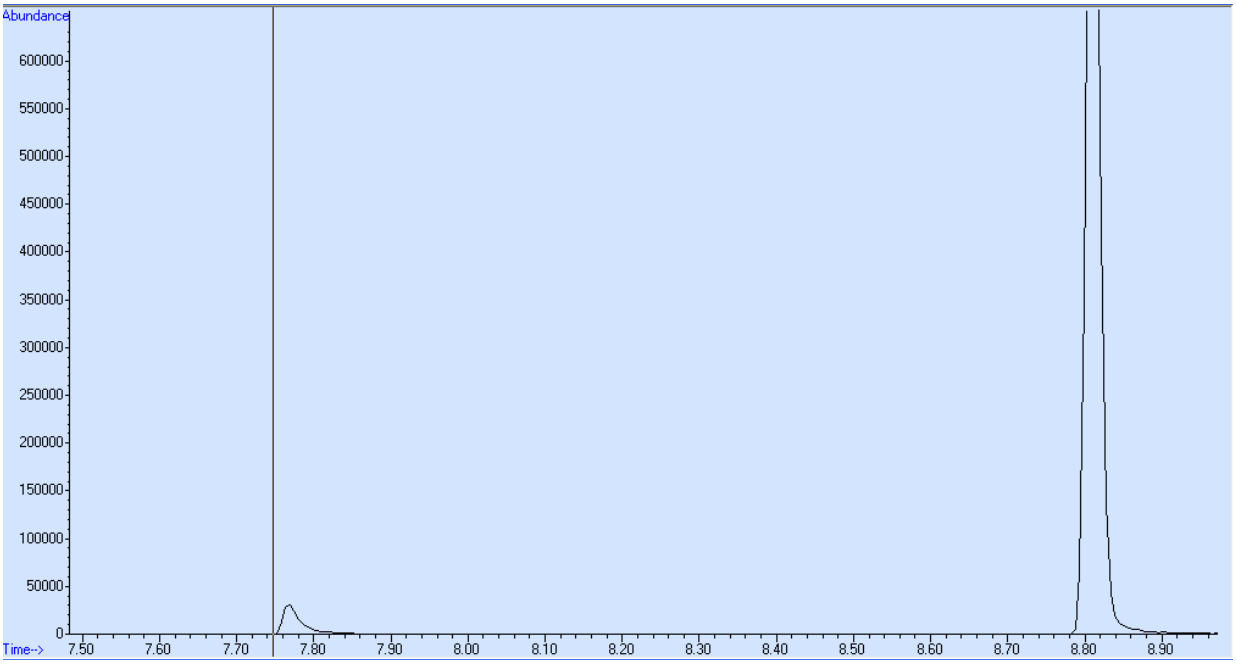

Figure S10. Gas chromatogram of the product mixture of PhOH oxidation. Left, BQ (7.77 min); right, PhOH (8.81 min).

Table S1. Benzoquinone (BQ) yield and selectivity as a function of $CuCl_2$ and NaCl concentrations after 12 h.

[$CuCl_2$] (μM)	[NaCl] (mM)	Yield (%)	Selectivity (%)
0	0	2.7	9
0	50	2.7	9
0	100	2.2	8
0	150	2.2	8
0	200	2.2	8
10	0	6.2	19
20	0	10.6	29
50	0	14.2	34
100	0	22.4	42
10	100	16	38
10	200	32	71
10	500	32	70
10	1000	32	68
10	1500	32	69
10	2000	36	83
10	2500	34	69
50	100	36	76

50	250	36	71
50	500	41	80
50	1000	38	85
50	1500	41	97
50	2000	45	99
100	100	46	83
100	200	45	93
100	400	45	87
100	1000	40	94

Reactions performed using [PhOH] = 1 mM and [H_2O_2] = 10 mM. [PhOH] and [BQ] were determined by deconvolution of UV absorbance at their respective λ_{max}, 270 and 288 nm, respectively.